Spatiotemporal discrete multicolor solitons

Zhiyong Xu,* Yaroslav V. Kartashov,† Lucian-Cornel Crasovan,‡ Dumitru Mihalache,‡ and Lluis Torner
ICFO-Institut de Ciencies Fotoniques, and Department of Signal Theory and Communications, Universitat Politecnica de Catalunya, 08034 Barcelona, Spain

(Received 16 February 2004; revised manuscript received 27 July 2004; published 20 December 2004)

We have found various families of two-dimensional spatiotemporal solitons in quadratically nonlinear waveguide arrays. The families of unstaggered odd, even, and twisted stationary solutions are thoroughly characterized and their stability against perturbations is investigated. We show that the twisted and even solitons display instability, while most of the odd solitons show remarkable stability upon evolution.

DOI: 10.1103/PhysRevE.70.066618 PACS number(s): 42.65.Tg, 42.65.Wi, 42.79.Gn

I. INTRODUCTION

Since their first experimental observation [1], quadratic solitons have been demonstrated in a variety of materials and geometries. Spatial, temporal, and spatiotemporal solitons in quadratic media have been extensively investigated both experimentally and theoretically (for detailed reviews, see [2–5]). Quadratic solitons also exist in the form of discrete entities, namely strongly localized wave packets forming in nonlinear waveguide arrays. Since their theoretical prediction in 1988 in cubic nonlinear media [6], discrete optical solitons have attracted a steadily growing interest because of their potential applications in switching and routing devices [7–9]. The discrete solitons that form in tight-coupled waveguide arrays made of quadratic nonlinear media have been comprehensively investigated [10–14] due to the rich variety of effects that are possible with them. It is noted that recently discrete quadratic solitons have been experimentally observed in arrays of waveguides made in lithium niobate [15]. Such richness may be further enhanced by combining the features of both continuous and discrete soliton families present in spatiotemporal discrete solitons, a possibility that we address here.

In the past two decades the concept of optical spatiotemporal solitons (STS's), referred to as light bullets in the three-dimensional case [16], has been attracting attention as a unique opportunity to create a self-supporting fully localized object. The existence of STS's in quadratic nonlinear materials was theoretically predicted [17] and thereafter experimentally realized in a two-dimensional geometry involving one temporal and one spatial coordinate [18]. The existence and properties of continuous-discrete spatiotemporal solitons have been extensively investigated in cubic nonlinear media and stable odd solitons have been shown to exist [19–23]. It was shown that the cubic weakly-coupled waveguide arrays act as collapse compressors [19–21]. In contrast with the cubic spatiotemporal solitons, the quadratic ones do not display collapse in both two- and three-dimensional geometries [24]. A still open problem, not analyzed so far, is the existence of space-time solitons in nonlinear waveguides with quadratic nonlinearity, that is, the existence of discrete spatiotemporal multicolor solitons.

In this paper we investigate in details the existence and stability of three representative families of two-dimensional spatiotemporal solitons in quadratic nonlinear waveguide arrays. We assume, in addition to the temporal dispersion of the pulse, the contribution of the discrete diffraction, that arises because of the weak coupling between neighboring waveguides.

Discrete soliton solutions were classified as *staggered* and *unstaggered* ones (see, for example, Ref. [25]). The staggered solutions display out-of-phase fields between the neighbor noncentral waveguides whereas the unstaggered ones display in-phase fields in these noncentral waveguides. Inside each of these classes of solitons (staggered and unstaggered) one can find solutions with different topologies, dictated mainly by the energy and phase distribution in the central waveguides. Thus, one can have (i) *odd* solitons, for which most part of the energy is located in one central waveguide and the energy distribution across the waveguide array is symmetric with respect to this central waveguide; (ii) *even* solitons, for which most part of the energy is equally distributed in the two central waveguides, the fields in these central waveguides being in-phase and of equal amplitudes; and (iii) *twisted* solitons, for which most part of the energy is equally distributed in the two central waveguides, but the fields in the two central waveguides are out-of-phase.

Here we will restrict ourselves to three representative families of continuous-discrete unstaggered solitons, namely the odd soliton [see Fig. 1(a)], the even soliton [see Fig. 1(c)] and the twisted soliton [see Fig. 1(d)]. Note that for the twisted soliton, the fundamental frequency field is, in fact, an antisymmetric one (the π jump of phase occurs only between the two central waveguides), whereas the second harmonic field is a symmetric one (having the form of an even discrete soliton). For all the solutions we deal with, the temporal profile, i.e., the shape of the pulses propagating in a specific waveguide, is a bell-shaped symmetric one [see Fig. 1(b), below]. Besides these stationary solutions, there exist a whole "zoology" of localized solutions, including staggered solitons, dark or dark-bright solitons, but their study is beyond the scope of the present work.

*Electronic address: Xu.Zhiyong@upc.es
†Also with the Physics Department, M. V. Lomonosov Moscow State University, Moscow, Russia.
‡Permanent address: Institute of Atomic Physics, Department of Theoretical Physics, P.O. Box MG-6, Bucharest, Romania.

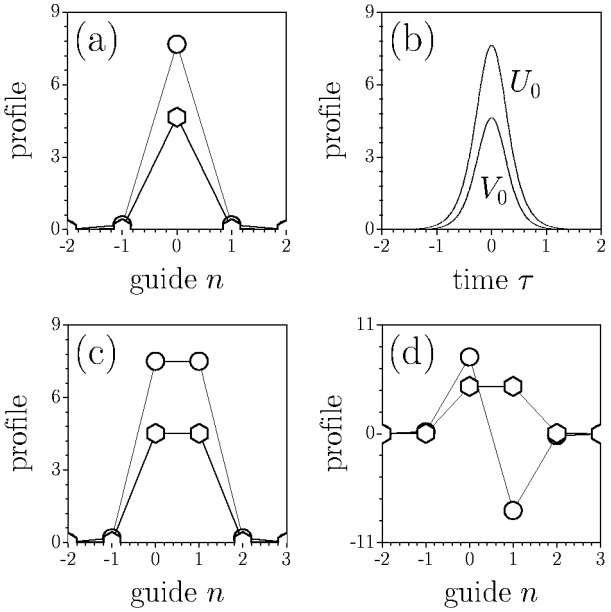

FIG. 1. Amplitude profiles of the (a) odd, (c) even, and (d) twisted solitons. Lines with circles show FF field; lines with hexagons show SH field. In (b) the time slice in the central waveguide ($n=0$) for odd soliton is shown. Even and twisted solitons feature the similar temporal profile. Here $C=0.1$, $b_1=3$, and $\beta=3$.

II. MODEL AND STATIONARY SOLUTIONS

The evolution of the spatiotemporal two-component field in quadratic nonlinear waveguide arrays in a degenerate second-harmonic generation geometry may be described by the following set of nonlinearly coupled reduced differential equations:

$$i\frac{\partial u_n}{\partial \xi} = -c_u(u_{n-1}+u_{n+1}) + \frac{g_1}{2}\frac{\partial^2 u_n}{\partial \tau^2} - u_n^* v_n \exp(-i\beta\xi),$$

$$i\frac{\partial v_n}{\partial \xi} = -c_v(v_{n-1}+v_{n+1}) + \frac{g_2}{2}\frac{\partial^2 v_n}{\partial \tau^2} - u_n^2 \exp(i\beta\xi), \quad (1)$$

where u_n and v_n represent the normalized amplitudes of the fundamental frequency (FF) and second-harmonic (SH) fields in the nth waveguide, with $n=-N,\ldots-1,0,1,\ldots,N$, $2N+1$ being the number of waveguides, the asterisk denotes complex conjugation, $c_{u,v}$ and $g_{1,2}$ are the linear coupling coefficients and group-velocity dispersion (GVD) coefficients, respectively, and β is the wave-vector mismatch. The evolution variable ξ denotes the normalized propagation distance along the waveguides. The dynamical system (1) admits several conserved quantities including the energy flow and Hamiltonian which read

$$I = \sum_n \int (|A_n|^2 + |B_n|^2)d\tau, \quad (2)$$

$$H = -\sum_n \int \left[\frac{g_1}{2}\left|\frac{\partial A_n}{\partial \tau}\right|^2 + c_u(A_n A_{n+1}^* + A_n^* A_{n+1}) + \frac{1}{2}(A_n^2)^* B_n + \frac{g_2}{4}\left|\frac{\partial B_n}{\partial \tau}\right|^2 + \frac{c_v}{2}(B_n B_{n+1}^* + B_n^* B_{n+1}) - \frac{\beta}{2}|B_n|^2 + \frac{1}{2}A_n^2 B_n^* \right] d\tau, \quad (3)$$

where we have defined $A_n \equiv u_n$, and $B_n \equiv v_n \exp(-i\beta\xi)$. The stationary solutions of Eqs. (1) have the form $u_n = U_n(\tau)\exp(ib_1\xi)$ and $v_n = V_n(\tau)\exp(ib_2\xi)$, where $U_n(\tau)$ and $V_n(\tau)$ are real functions, and $b_{1,2}$ are real propagation constants verifying $b_2 = 2b_1 + \beta$. Continuous-discrete solitons arise from a balance between discrete diffraction, dispersion and quadratic nonlinearity. The families of odd, even, and twisted stationary continuous-discrete solitons have been obtained numerically by a standard relaxation method. For given coupling strengths $c_{u,v}$, dispersions $g_{1,2}$ and wave-vector mismatch β, the soliton families are parametrized by the nonlinear wave number shift b_1. The coupling coefficients $c_{u,v}$ were considered positive, and equal, so further we introduce single parameter C to describe coupling between neighboring guiding sites. Throughout this paper we will always consider anomalous dispersions at both frequencies and we fixed $g_1=-0.25$ and $g_2=-0.5$. Note that in the continuous case, long-lived solitonlike propagation when the GVD is slightly normal at SH is known to occur [26,27]; thus a similar behavior might occur in the continuous-discrete spatiotemporal case analyzed here.

In Figs. 2(a) and 2(b) we show the dependencies of the peak amplitude A_u and the temporal full width at half maximum of the pulse in the central waveguide W_u as a function of the coupling coefficient C for a fixed wave number b_1 at phase matching ($\beta=0$). Note that with increase of coupling strength amplitude of odd and even solitons monotonically decreases and their width increases, whereas the amplitude and width of the twisted solitons are the nonmonotonic function of C. This is illustrated also in Fig. 3 where profiles of odd solitons $|U_n(\tau)|$ at two different coupling constants are shown. Note that with increase of coupling constant soliton covers more guiding sites, while at $C\to 0$ it is located primarily in the central guiding site.

Similar to the two-dimensional (continuous-continuous) solitons in uniform media, there exist cutoff b_{co} of the nonlinear wave number shift b_1 depending on the sign and absolute value of the mismatch parameter β. Moreover, as we have an additional degree of freedom, namely the discrete spatial coordinate, we have investigated the dependence of the cutoff wave number b_{co} on the coupling coefficient C for a given wave-vector mismatch. For a phase-matched geometry ($\beta=0$), we have obtained almost linear dependencies of the cutoff wave number on the coupling coefficients for all three families of solutions we deal with [see Fig. 2(c)]. Note that cutoffs for odd and even solitons are equal. As a general rule, the stronger the coupling, the larger the cutoff wave number b_{co}. When $C=0$ we got $b_{co}=0$, thus recovering the known result for the continuous quadratic solitons: $b_{co} = \max\{-\beta/2, 0\}$.

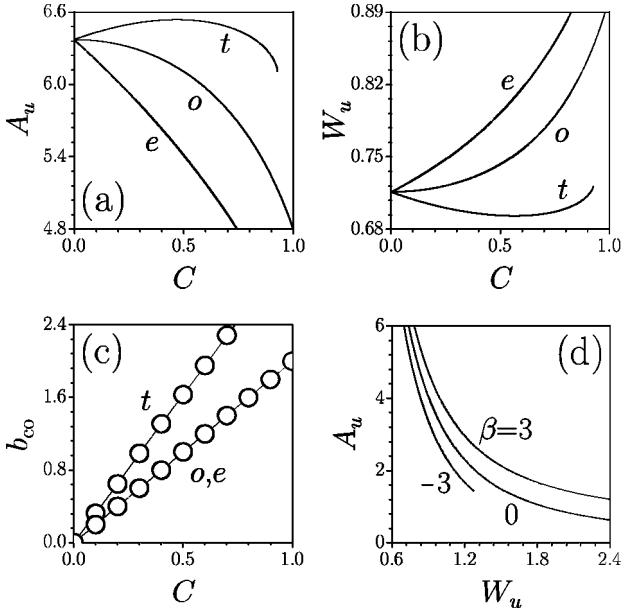

FIG. 2. (a) Peak amplitude and (b) temporal width of FF wave in the central waveguide for odd, even, and twisted solitons versus coupling coefficient at $b_1=3$ and $\beta=0$. (c) Wave number cutoff versus coupling coefficient at $\beta=0$. The symbols "*o*," "*e*," and "*t*" stand for the odd, even, and twisted solitons, respectively. (d) FF wave amplitude versus temporal width in the central waveguide for odd soliton at $C=0.1$ and different phase mismatches. Only stable branch has been plotted for negative β.

We also have investigated the peak amplitude and the temporal width in the central waveguide for odd, even and twisted continuous-discrete solitons as functions of the wave-vector mismatch for fixed nonlinear wave number shift b_1 and linear coupling coefficient C. The solitons that form at larger phase mismatches have larger amplitudes and are narrower than those forming at smaller phase mismatches. This feature was observed for one- and two-dimensional continuous solitons in quadratic media for which at phase matching the product (peak amplitude)$\times$(width^2) is a constant quantity [28]. In Fig. 2(d) we plot the amplitude of the stationary odd soliton as function of its temporal width. We see that outside phase-matching the families of solitons exhibit a more complicated amplitude-width relationship, similar to the case of continuous quadratic solitons [28]. The scaling properties of Eqs. (1) can be written as

$$u_n=\psi\tilde{u}_n,\quad v_n=\psi\tilde{v}_n,\quad b_1=\psi\tilde{b}_1,$$
$$\beta=\psi\tilde{\beta},\quad \tau=\psi^{-1/2}\tilde{\tau},\quad I=\psi^{3/2}\tilde{I},\qquad (4)$$

where ψ being the scaling parameter.

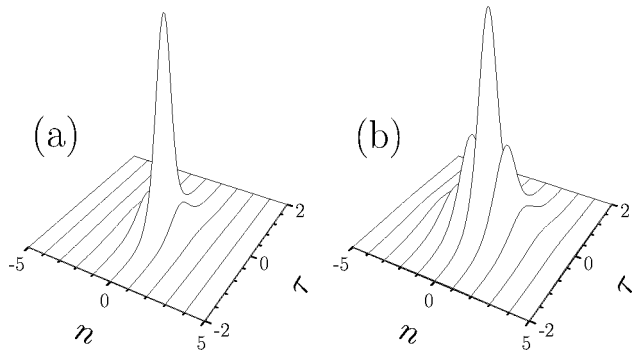

FIG. 3. Profiles of odd solitons for (a) $C=0.5$ and (b) $C=1$ at $b_1=3$, $\beta=0$. Only the modulus of the amplitude of the FF wave is shown. The SH shows similar features.

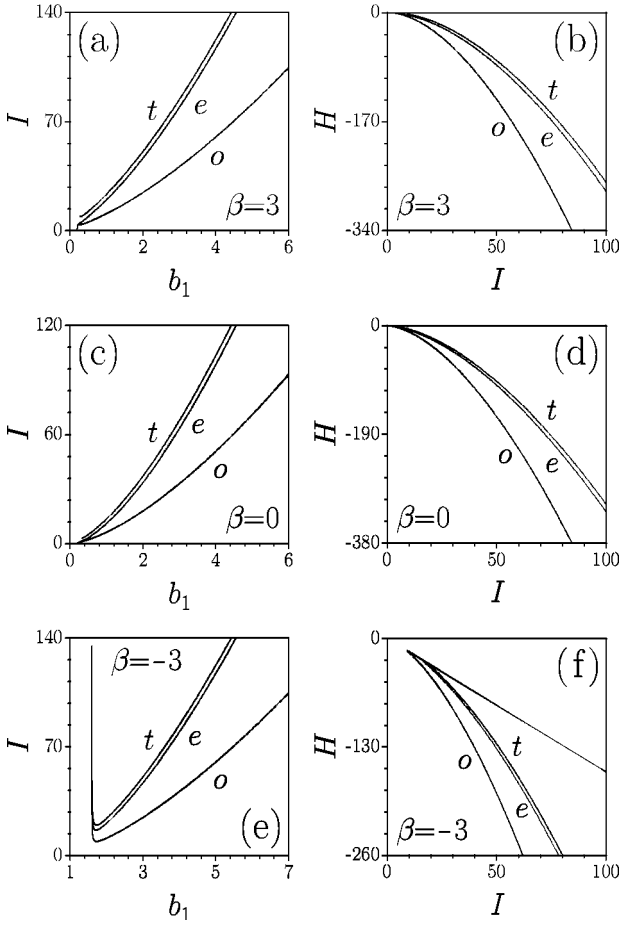

FIG. 4. Energy flow versus wave number and Hamiltonian versus energy flow for odd, even, and twisted solitons at three representative values of phase mismatch and $C=0.1$. The labels are the same as in Figs. 2.

In Figs. 4(a)–4(f) we have represented the dependencies energy flow I–wave number b_1 (left column) and Hamiltonian H–energy flow I (right column) that give us a deeper insight into the properties of continuous-discrete soliton families. One can see that odd solitons realize the minimum of Hamiltonian for a given energy flow, thus they are expected to be the most robust on propagation. The Peierls-Nabarro potential, that is the difference between Hamiltonian of the odd soliton and that of the even one [29], corresponding to the same energy flow, is negative everywhere. From a geometrical point of view, this would mean that odd solitons are stable in the entire domain of their existence [30]. Our numerical simulations, described in detail in the next section, show that, indeed, this is the case except for solitons at negative phase mismatches that are unstable only in a narrow region near cutoff [see Fig. 5(a)] [28,31].

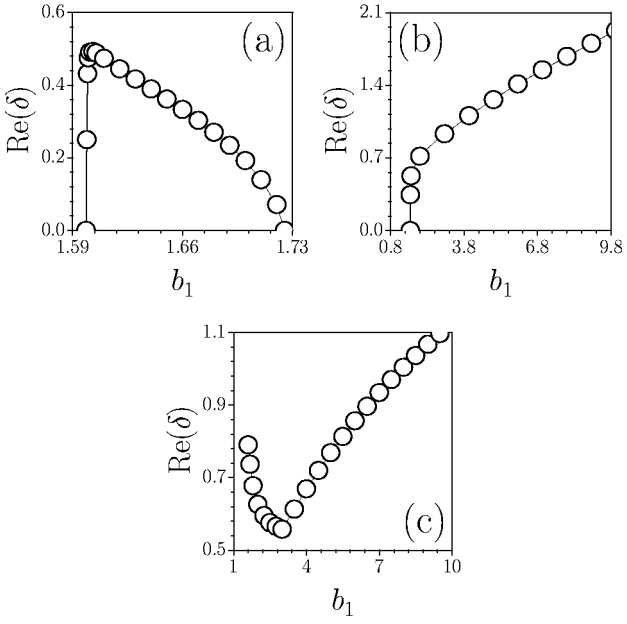

FIG. 5. Growth rate versus wave number for (a) odd, (b) even, and (c) twisted solitons at $\beta=-3$ and $C=0.1$.

III. STABILITY ANALYSIS

A key issue concerning the soliton families we found is their stability on propagation. In order to elucidate if the localized continuous-discrete solitons are dynamically stable we have performed both a linear stability analysis and direct numerical simulations. We seek for perturbed solution of Eq. (1) in the form

$$u_n(\tau,\xi) = [U_n(\tau) + \mu f_n(\tau,\xi)]\exp(ib_1\xi),$$

$$v_n(\tau,\xi) = [V_n(\tau) + \mu h_n(\tau,\xi)]\exp[i(2b_1+\beta)\xi]. \qquad (5)$$

Here μ is a small parameter, $U_n(\tau)$ and $V_n(\tau)$ are the stationary solutions and $f_n(\tau,\xi)$ and $h_n(\tau,\xi)$ are the perturbations. Then after linearizing the evolution equations (1) we are left with a system of linear coupled differential equations for the perturbations (see, e.g., Ref. [32]):

$$i\frac{\partial f_n}{\partial \xi} = -c_u(f_{n-1}+f_{n+1}) + \frac{g_1}{2}\frac{\partial^2 f_n}{\partial \tau^2} - (U_n^* h_n + V_n f_n^*) + b_1 f_n,$$

$$i\frac{\partial h_n}{\partial \xi} = -c_v(h_{n-1}+h_{n+1}) + \frac{g_2}{2}\frac{\partial^2 h_n}{\partial \tau^2} - 2U_n f_n + (2b_1+\beta)h_n. \qquad (6)$$

We have solved both this linear system and the nonlinear dynamical equations (1) with a combined fast-Fourier transform, to deal with the linear differential part in the temporal coordinate, and a fourth-order Runge-Kutta method, to deal with the cross-coupling terms. We have typically used 512 or 1024 points in the time domain and we have considered tens of array sites (e.g., 61), depending on the width of the solution whose stability is investigated. The step length along the propagation coordinate was of the order of 10^{-3}. The accuracy of the results was checked by doubling the number of points in the transverse coordinate and by halving the propagation step. As another check for the evolution equations (1) we have verified the conservation of the prime integrals (energy flow I and Hamiltonian H). In order to let the radiation to escape from the computation window we have implemented transparent (absorbing) boundary conditions.

We have determined the dominant eigenvalue δ of the linearized problem using the same approach as in Ref. [32]. The method gives us only the dominant eigenvalue, not the whole eigenvalue spectrum. This eigenvalue corresponds to the most rapidly (exponentially) developing instability. The noisy perturbation we consider at $\xi=0$ develops, during evolution, to a localized eigenvector with a well defined symmetry, depending on the type of the solution considered. In the cases where an instability was detected, only real instability eigenvalues were found. The dominant eigenvalue was calculated in the form

$$\mathrm{Re}(\delta) = \frac{1}{2\Delta\xi}\log\left\{\left(\sum_n \int_{-\infty}^{\infty}[|f_n(\tau,\xi+\Delta\xi)|^2 + |h_n(\tau,\xi+\Delta\xi)|^2]d\tau\right) \times\left(\sum_n \int_{-\infty}^{\infty}[|f_n(\tau,\xi)|^2 + |h_n(\tau,\xi)|^2]d\tau\right)^{-1}\right\}. \qquad (7)$$

This dominant eigenvalue tends to zero when one approaches the stability region. The results we got for the growth rate calculations at negative phase mismatch ($\beta=-3$) are summarized in Fig. 5. They indicate instability for even and twisted solitons [10] and a stability region for odd solitons which starts at $b_1^{stab}\approx 1.725$. This result is in good agreement with the direct simulations of evolution Eq. (1). For positive wave-vector mismatches or at phase-matching the growth rate calculations indicate instability for even and twisted solitons and complete stability for odd solitons.

Our calculations show that odd continuous-discrete solitons obey the Vakhitov-Kolokolov stability criterion [33], i.e., they are stable provided $dI/db_1>0$, and unstable, otherwise. The Vakhitov-Kolokolov criterion was shown also to hold for discrete space-time solitons that exist in Kerr nonlinear media [22,23]. Moreover, the unstable odd cubic continuous-discrete solitons can display collapse-type instabilities, a reminiscent feature of the two-dimensional stationary solutions of nonlinear Schrödinger equation, while the unstable quadratic discrete space-time odd solitons do not display this type of instability [24].

Let us stress that as compared to the one-dimensional discrete twisted solitons forming in quadratic media that can be stable in specific parameter regions, in our case, the introduction of a time coordinate leads to the destabilization of these solutions. However, one of the central points of this work is that we found families of stable odd continuous-discrete multicolor solitons. As illustrated in Fig. 6(b), stable odd solitons can propagate for huge distances without altering their shape and eliminating the added random white noise during evolution. The case shown here corresponds to

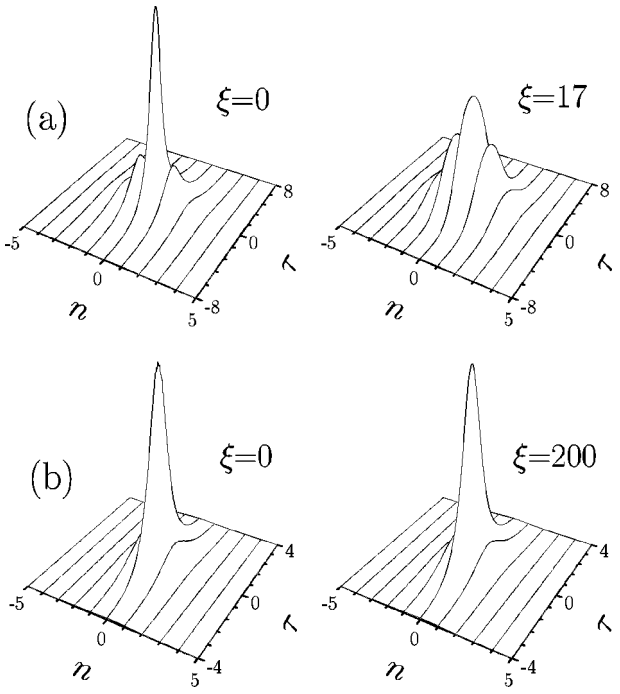

FIG. 6. (a) Propagation of unstable odd soliton corresponding to $b_1=1.65$ in the presence of small perturbation found upon linear stability analysis. Perturbation amplitude $\mu=0.01$. (b) Propagation of stable odd soliton at $b_1=1.735$ in the presence of white noise with variance $\sigma^2_{noise}=0.01$. Only the modulus of the amplitude of the SH wave is shown, at different propagation distances. Plots in left and right columns are shown with the same scale for easier comparison. Phase mismatch $\beta=-3$ and coupling constant $C=0.1$.

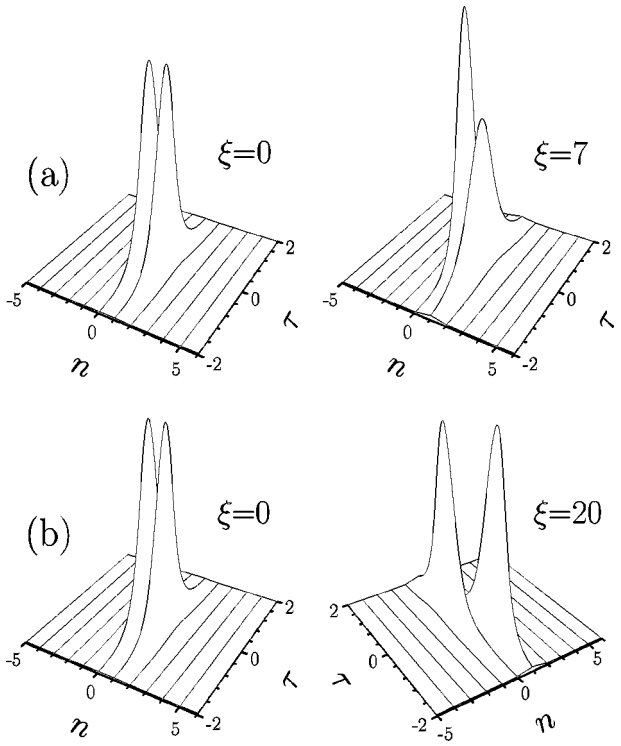

FIG. 7. Propagation of unstable even (a) and twisted (b) solitons corresponding to $b_1=3$ in the presence of small perturbations found upon the linear stability analysis. Perturbation amplitude $\mu=0.01$. Only the modulus of the amplitude of the SH wave is shown, at different propagation distances. Plots in left and right columns are shown with the same scale for easier comparison. Phase mismatch $\beta=-3$ and coupling constant $C=0.1$.

negative wave-vector mismatch $\beta=-3$ but similar stable evolution has been obtained for positive mismatches and phase-matching geometries except for odd solitons from the branch where $dI/db_1<0$, which are unstable and will therefore decay after a finite propagation distance [see Fig. 6(a)].

In addition, we also thoroughly investigated the decay scenarios of the other two types of solitons: even and twisted. As stated before we have not observed any stable even or twisted continuous-discrete soliton. Figure 7 shows possible instability scenarios for unstaggered even and unstaggered twisted solitons. We have found that a perturbed even soliton typically tranforms into an odd one through increasing field oscillation in neighboring waveguides [Fig. 7(a)], and perturbed twisted soliton usually splits into two solitons which fly apart as when a repulsive force would act between them [Fig. 7(b)]. We have observed a π phase difference between the formed odd solitons and this could explain the repulsive force between them. Note that during the splitting process the resulting odd solitons are still locked in a specific waveguide, but they are allowed to repel in time. This unique feature comes with discreteness which does not allow the soliton energy to escape from the waveguide where it was initially located.

IV. CONCLUSION

We have shown that stable, spatiotemporal continuous-discrete solitons are possible in quadratic nonlinear waveguide arrays. Families of unstaggered odd, even and twisted stationary solutions have been found and thoroughly characterized. The linear stability analysis is in agreement with the direct simulations indicating that the odd continuous-discrete solitons obey the Vakhitov-Kolokolov stability criterion. The salient point put forward is that most of the spatiotemporal unstaggered odd solitons are stable against perturbations. This result is important in view of the generation of discrete solitons with pulsed light in the context of the exploration of their potential application to switching schemes [7–9].

ACKNOWLEDGMENTS

This work was partially supported by the Generalitat de Catalunya, Institució Catalana de Recerca i Estudis Avancats (ICREA), Barcelona, and by the Spanish Government through grant BFM2002-2861.

[1] W. E. Torruellas, Z. Wang, D. J. Hagan, E. W. VanStryland, G. I. Stegeman, L. Torner, and C. R. Menyuk, Phys. Rev. Lett. **74**, 5036 (1995).
[2] G. I. Stegeman, D. J. Hagan, and L. Torner, Opt. Quantum Electron. **28**, 1691 (1996).
[3] C. Etrich, F. Lederer, B. A. Malomed, T. Peschel, and U. Peschel, Prog. Opt. **41**, 483 (2000).
[4] A. V. Buryak, P. Di Trapani, D. V. Skryabin, and S. Trillo, Phys. Rep. **370**, 63 (2002).
[5] L. Torner and A. Barthelemy, IEEE J. Quantum Electron. **39**, 22 (2003).
[6] D. N. Christodoulides and R. I. Joseph, Opt. Lett. **13**, 794 (1988).
[7] D. N. Christodoulides, F. Lederer, and Y. Silberberg, Nature (London) **424**, 817 (2003).
[8] F. Lederer and Y. Silberberg, Opt. Photonics News **13**, 49 (2002).
[9] O. Bang and P. D. Miller, Opt. Lett. **21**, 1105 (1996).
[10] A. A. Sukhorukov, Y. S. Kivshar, O. Bang, and C. M. Soukoulis, Phys. Rev. E **63**, 016615 (2000).
[11] O. Bang, P. L. Christiansen, and C. B. Clausen, Phys. Rev. E **56**, 7257 (1997).
[12] P. D. Miller and O. Bang, Phys. Rev. E **57**, 6038 (1998).
[13] T. Peschel, U. Peschel, and F. Lederer, Phys. Rev. E **57**, 1127 (1998).
[14] A. Kobyakov, S. Darmanyan, T. Pertsch, and F. Lederer, J. Opt. Soc. Am. B **16**, 1737 (1999); B. A. Malomed, P. G. Kevrekidis, D. J. Frantzeskakis, H. E. Nistazakis, and A. N. Yannacopoulos, Phys. Rev. E **65**, 056606 (2002).
[15] R. Iwanow, R. Schiek, G. I. Stegeman, T. Pertsch, Y. Min, and W. Sohler, Phys. Rev. Lett. **93**, 113902 (2004).
[16] Y. Silberberg, Opt. Lett. **15**, 1282 (1990).
[17] A. A. Kanashov and A. M. Rubenchik, Physica D **4**, 122 (1981); B. A. Malomed, P. Drummond, H. He, A. Berntson, D. Anderson, and M. Lisak, Phys. Rev. E **56**, 4725 (1997); D. V. Skryabin and W. J. Firth, Opt. Commun. **148**, 79 (1998); D. Mihalache, D. Mazilu, B. A. Malomed, and L. Torner, *ibid.* **152**, 365 (1998); D. Mihalache, D. Mazilu, J. Dörring, and L. Torner, *ibid.* **159**, 129 (1999); D. Mihalache, D. Mazilu, L.-C. Crasovan, L. Torner, B. A. Malomed, and F. Lederer, Phys. Rev. E **62**, 7340 (2000); L. Torner, S. Carrasco, J. P. Torres, L.-C. Crasovan, and D. Mihalache, Opt. Commun. **199**, 277 (2001).
[18] X. Liu, L. J. Qian, and F. W. Wise, Phys. Rev. Lett. **82**, 4631 (1999).
[19] A. B. Aceves, C. De Angelis, A. M. Rubenchik, and S. K. Turitsyn, Opt. Lett. **19**, 329 (1994).
[20] A. B. Aceves, C. De Angelis, G. G. Luther, and A. M. Rubenchik, Opt. Lett. **19**, 1186 (1994).
[21] A. B. Aceves, G. G. Luther, C. De Angelis, A. M. Rubenchik, and S. K. Turitsyn, Phys. Rev. Lett. **75**, 73 (1995).
[22] E. W. Laedke, K. H. Spatschek, and S. K. Turitsyn, Phys. Rev. Lett. **73**, 1055 (1994).
[23] E. W. Laedke, K. H. Spatschek, S. K. Turitsyn, and V. K. Mezentsev, Phys. Rev. E **52**, 5549 (1995).
[24] L. Berge, V. K. Mezentsev, J. J. Rasmussen, and J. Wyller, Phys. Rev. A **52**, R28 (1995).
[25] F. Lederer, S. Darmanyan, and A. Kobyakov, in *Spatial Solitons*, edited by S. Trillo and W. Torruellas, Springer Series on Optical Sciences (Springer, New York, 2001).
[26] L. Torner, IEEE Photonics Technol. Lett. **11**, 1268 (1999).
[27] I. N. Towers, B. A. Malomed, and F. W. Wise, Phys. Rev. Lett. **90**, 123902 (2003).
[28] L. Torner, D. Mihalache, D. Mazilu, and N. N. Akhmediev, Opt. Lett. **20**, 2183 (1995); L. Torner, D. Mihalache, D. Mazilu, E. M. Wright, W. E. Torruellas, and G. I. Stegeman, Opt. Commun. **121**, 149 (1995).
[29] Yu. S. Kivshar and D. K. Campbell, Phys. Rev. E **48**, 3077 (1993).
[30] D. Cai, A. R. Bishop, and N. Gronbech-Jensen, Phys. Rev. Lett. **72**, 591 (1994).
[31] D. E. Pelinovsky, A. V. Buryak, Y. S. Kivshar, Phys. Rev. Lett. **75**, 591 (1995).
[32] J. M. Soto-Crespo, D. R. Heatley, E. M. Wright, and N. N. Akhmediev, Phys. Rev. A **44**, 636 (1991); D. V. Skryabin and W. J. Firth, Phys. Rev. E **58**, 3916 (1998); D. Mihalache, D. Mazilu, L.-C. Crasovan, I. Towers, B. A. Malomed, A. V. Buryak, L. Torner, and F. Lederer, *ibid.* **66**, 016613 (2002).
[33] M. G. Vakhitov and A. A. Kolokolov, Izv. Vyssh. Uchebn. Zaved., Radiofiz. **16**, 1020 (1973) [Radiophys. Quantum Electron. **16**, 783 (1973)].